#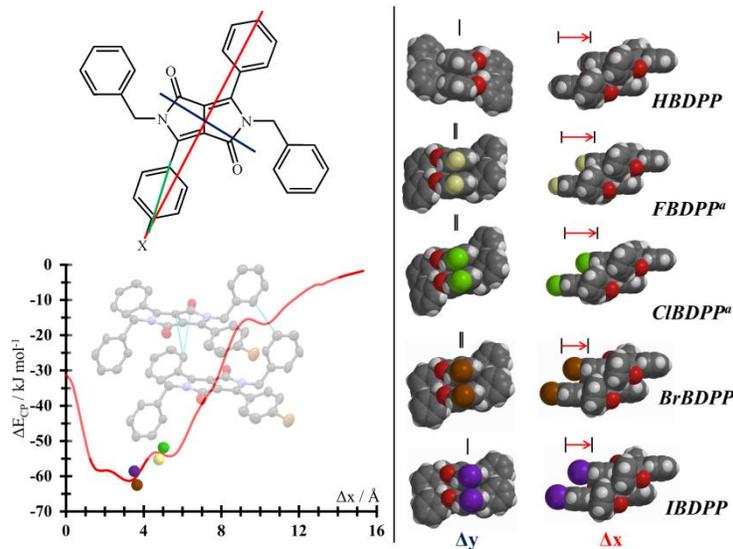 Intermolecular interactions and energetics in the crystalline π-π stacks and associated model dimer systems of asymmetric halogenated diketopyrrolopyrroles

Jesus Calvo-Castro,*[a] *Monika Warzecha,*[b] *Iain D.H. Oswald,*[b] *Alan R. Kennedy,*[c] *Graeme Morris,*[a] *Andrew J. McLean*[a] *and Callum J. McHugh**[a]

[a]School of Science and Sport, University of the West of Scotland, Paisley, PA1 2BE, UK.
[b]Strathclyde Institute of Pharmacy and Biomedical Sciences, University of Strathclyde, Glasgow, G1 1XL, UK.

ABSTRACT: Four novel structurally analogous asymmetric, halogenated N-benzyl substituted diketopyrrolopyrroles (DPP) have been synthesised and their crystal structures obtained. All four structures exhibit π-π stacks with very small displacements along their short molecular axes, which is a characteristic of N-benzyl substitution. Intermolecular interaction energies were computed for extracted crystal π-π dimer pairs using density functional theory to investigate the most energetically favoured position of the halogen atoms in **FBDPP** and **ClBDPP** structures. Effective stabilisation energies arising from both benzyl and halogen substitution in these derivatives and in **BrBDPP** and **IBDPP** π-π dimer pairs were also determined to probe the impact of these groups on dimer stability. Effects of the intermonomer displacements along the long molecular axis, which have been shown by us previously to significantly influence wavefunction overlap and effective electronic coupling, were investigated in detail using aligned and anti-aligned model systems of **ClDPP** and **BrDPP**. The predictions of these model systems are remarkably consistent with the observed displacements in their crystal derived π-π dimer pair equivalents, offering insight into the effective role of intermolecular contacts in stabilising crystal structures involving this DPP molecular motif.

Dr. C. J. McHugh*
University of the West of Scotland
School of Science and Sport
Paisley, UK
PA1 2BE
Tel: +44 (141) 848 3210
Fax: +44 (141) 848 3204
Email: callum.mchugh@uws.ac.uk

Intermolecular interactions and energetics in the crystalline π-π stacks and associated model dimer systems of asymmetric halogenated diketopyrrolopyrroles

Jesus Calvo-Castro,[a] *Monika Warzecha,*[b] *Iain D.H. Oswald,*[b] *Alan R. Kennedy,*[c] *Graeme Morris,*[a] *Andrew J. McLean*[a] *and Callum J. McHugh*[a]*

[a]School of Science and Sport, University of the West of Scotland, Paisley, PA1 2BE, UK.

[b]Strathclyde Institute of Pharmacy and Biomedical Sciences, University of Strathclyde, Glasgow, G1 1XL, UK.

[c]Department of Pure & Applied Chemistry, University of Strathclyde, Glasgow G1 1XL, UK.

*Corresponding authors: jesus.calvo@uws.ac.uk, callum.mchugh@uws.ac.uk

ABSTRACT: Four novel structurally analogous asymmetric, halogenated N-benzyl substituted diketopyrrolopyrroles (DPP) have been synthesised and their crystal structures obtained. All four crystal structures exhibit π-π stacks with very small displacements along their short molecular axis, which based upon our previous studies involving symmetrical DPPs is a characteristic of N-benzyl substitution. Intermolecular interaction energies were computed for extracted crystal π-π dimer pairs by means of M06-2X density functional at 6-311G(d) level to investigate the

most energetically favoured position of the halogen atoms in **_FBDPP_** and **_ClBDPP_** structures. In addition, effective stabilisation energies arising from both benzyl and halogen substitution in these derivatives and in **_BrBDPP_** and **_IBDPP_** π-π dimer pairs were determined in order to probe the impact of these groups on the resulting dimer stability. Effects of the intermonomer displacements along the long molecular axis, which have been shown by us previously to significantly influence wavefunction overlap and effective electronic coupling, were investigated in detail using aligned and anti-aligned model systems of **ClDPP** and **BrDPP**. The predictions of these model systems are remarkably consistent with the observed displacements in their crystal derived π-π dimer pair equivalents, offering insight into the effective role of intermolecular contacts in crystal structures involving this molecular motif, particularly with a view towards crystal engineering in these systems. As a result, we believe that this study should be of significant interest to the growing DPP based materials community and in general to those investigating the detailed manner by which substituents can be employed in the supramolecular design of crystalline molecular architectures.

INTRODUCTION

Diketopyrrolopyrroles (DPPs) are widely employed in industry as high performance pigments on account of their desirable properties such as brightness, low solubility and light and weather fastness.[1-5] More recently there has been an increasingly large surge of interest in DPP based materials employed as charge transfer mediators in functional devices, either in the form of small molecules or polymers.[6-17] Currently, we are engaged in the in-depth investigation and rational design of crystalline small molecule DPPs, specifically to develop an understanding of their behaviour and application in optical and optoelectronic environments.[18-20] We are particularly interested in the exploitation of structure-property relationships involving these materials,[19,20]

targeted towards rational design of functional charge transfer mediating materials. Previous studies of N-substituted DPP single crystal systems[19-22] have shown that they tend to crystallise forming slipped π-π stacking interactions and not the characteristic herringbone crystal structures observed in non-substituted acenes, thiophenes[23-26] or DPP pigments[27-29]. In such systems it is crucial to optimise intermonomer displacements along the short and long molecular axes via judicious molecular design in order to achieve optimum intermolecular interactions as well as wavefunction overlap, which is critical for effective charge transport.[19,26,30-32] Given the high sensitivity of hole (t_h) and electron (t_e) transfer integrals to small intermolecular displacements, it is also desirable to maximise thermal integrity with respect to intermonomer slip by optimising the strength of intermolecular interactions in π-conjugated systems.[19,26,31,33] Understanding the nature of non-covalent intermolecular interactions in π-conjugated systems and how these interactions can be modified via systematic and rational substitution is therefore of fundamental importance in advancing the design of supramolecular architectures in crystal engineering as well as in drug design and biological probes. Consequently, studies such as the one presented herein are important in providing a deeper insight into the manner by which substituents can be employed in supramolecular design.

The nature of the intermolecular interactions stabilising π-conjugated systems is of considerable recent interest.[34-60] The π-resonance based model proposed by Hunter and Sanders[34,35,38,39] and the π/polar model of Cozzi and Siegel[36,37] have been shown to inaccurately represent intermolecular interactions between π-conjugated architectures since they neglect the crucial role played by dispersion effects in this type of interaction. Recent studies by Wheeler and Houk[48,49,55,60] and Sherrill and co-workers (using symmetry-adapted perturbation theory)[41-44,52-54] have shown that π-π dimers in benzene derived pairs are primarily stabilised via local bond

dipole/bond dipole and induced bond dipole interactions rather than HOMO/LUMO based donor-acceptor global charge transfer type interaction suggested previously. Despite this progress, there is a clear lack of experimental studies[34,55,61-64] which test these theoretical predictions, particularly in relation to their influence on those interactions which are derived from crystal structures and associated model systems. Importantly, dispersion interactions denote the main point of discrepancy between experimental and theoretical results, given that most experimental work has been conducted in solution where electrostatic effects are dominant.[38,55,65]

Herein, we aim to enhance the understanding of the impact of structural variation on the π-π stacking interactions in crystalline DPP systems by reporting the synthesis, determination and characterisation of four asymmetric mono-halogenated N-substituted DPP single crystal structures (Scheme 1), that systematically vary in only one atom out of sixty, located at the para position of one of the two phenyl rings linked to the central DPP core. Previously, we have highlighted the effect of varying both halogen atoms on the intermolecular interaction energies and charge transfer integrals in a series of symmetric di-halogenated DPP single crystal structures. In the following report, we examine, in essence, "real" cropped equivalents from our initial study, thus facilitating a deeper understanding of the effective influence of the additional halogen atom on the important π-π stacking interactions and their associated energetics. The four reported structures were given names with a form of **XYDPP** arising from their topology where **X** and **Y** denote the substitution on the para position of one out of the two phenyl rings attached the central DPP core and the lactam nitrogen atoms respectively. These four structures were based on fluoro (*FBDPP*), chloro (*ClBDPP*), bromo (*BrBDPP*) and iodo (*IBDPP*) substituted DPPs (with *B* = N-benzyl substitution). The particular interest in halogen substitution can be readily understood from the enhanced optoelectronic behaviour observed in materials containing

these groups[66,67] as well as the potential for mono-halogenated DPP based materials to be employed as an interesting platform for the further synthesis of structurally related systems.[20]
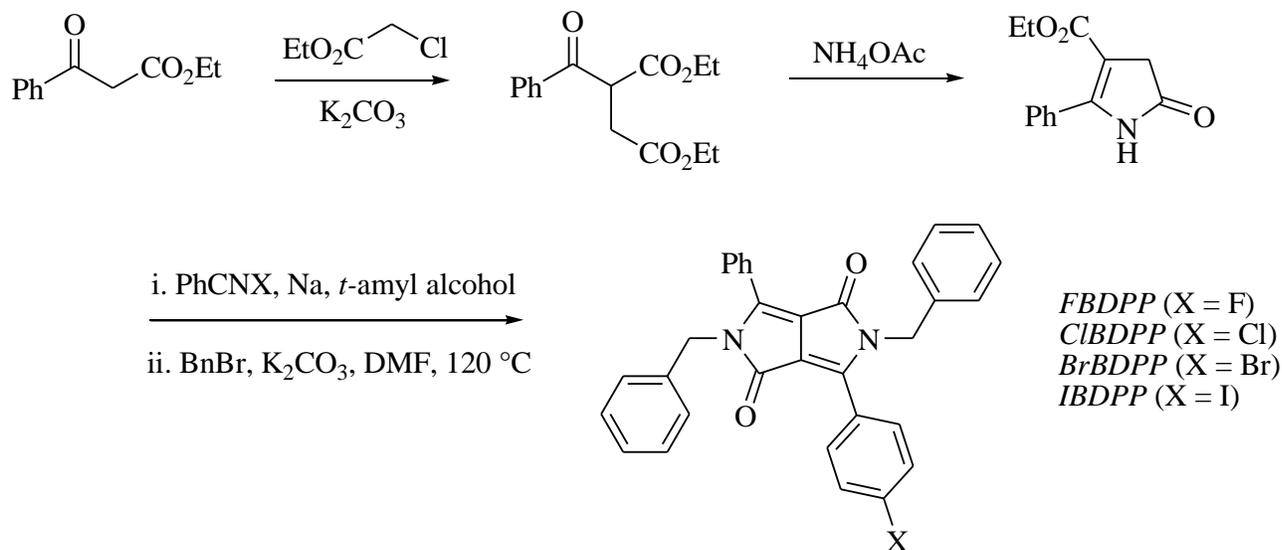
Scheme 1. Synthesis of asymmetric mono-halogenated DPPs.

EXPERIMENTAL SECTION

Reagents and instrumentation. Unless otherwise specified, all starting materials and reagents were purchased from Sigma-Aldrich and used as received without further purification. ^{1}H NMR and ^{13}C NMR spectra were determined using a JEOL ECS400 400 MHz spectrometer (in CDCl$_3$). Elemental analyses were carried out using the service provided at Jagiellonian University in Krakow, Poland. FTIR analyses were carried out on the neat samples by attenuated total reflectance using a PerkinElmer Spectrum One FTIR Spectrometer with Universal ATR Sampling Accessory.

Synthesis. 2,3-Dihydro-2-oxo 5-phenyl-1H-pyrrole-4-carboxylic acid ethyl ester (**Pyrroline ester**).[68] A suspension of ethyl benzoylacetate (20.2 g, 18.3 ml, 105 mmol), K$_2$CO$_3$ (15.2 g, 110

6

mmol), NaI (2.0 g), and ethyl chloroacetate (13.2 g, 11.6 ml, 108 mmol) in acetone/DME 120 ml:80 ml was heated under reflux for 24 hours. After cooling to room temperature the salts were filtered and washed with acetone. The combined filtrates were evaporated to dryness under reduced pressure affording an oily, brown intermediate product with sufficient purity for the next stage of the preparation. The crude product was dissolved in a mixture of acetic acid (200 ml) and ammonium acetate (78.7 g, 1.02 mol) and the reaction mixture was then stirred at reflux for 3 hours. After cooling to room temperature, the reaction mixture was added to ice-water (800 ml). The precipitate was filtered and washed with water. The residue was recrystallized from ethanol/water 4:1. After drying under reduced pressure the title product (17.87 g, 73 % starting from benzoylacetate) was obtained as a white-grey powder. ^{1}H NMR (400 MHz, CDCl$_3$): 1.15-1.19 (t, 3H, CH$_3$), 3.49 (s, 2H, CH$_2$), 4.08-4.14 (q, 2H, CH$_2$), 7.42–7.45 (m, 3H, ArH), 7.59–7.62 (m, 2H, ArH), 8.49 (br s, 1H, NH). ^{13}C NMR: 14.5 (CH$_3$), 39.1 (CH$_2$), 60.4 (CH$_2$), 105.0 (C=C), 128.6 (C=C), 129.1 (C=C), 130.0 (C=C), 130.9 (C=C), 151.6 (C=C), 163.6 (C=O), 177.5 (C=O). Melting point: 173-175 °C.

3-(4-fluorophenyl)-6-phenylpyrrolo[3,4-c]pyrrole-1,4(2H,5H)-dione (**FDPP**). Under nitrogen atmosphere and vigorous stirring 4-fluorobenzonitrile (0.32 g, 2,7 mmol) and the pyrroline ester (0.45 g, 1.96 mmol) were added to a solution of sodium t-amyloxide (obtained from 0.14 g, 6.1 mmol sodium metal dissolved in 20 ml dry t-amyl alcohol). The colour changed to dark red and a red solid precipitated. The mixture was stirred under reflux for 2hours. After cooling, 20 ml of ice-cold methanol with 2 ml of hydrochloric acid were added. The red precipitate was filtered, washed with methanol and water and then dried under vacuum to give **FDPP** as a bright red powder (0.22 g, 37 % yield), which was used without further purification or characterisation.

3-(4-chlorophenyl)-6-phenylpyrrolo[3,4-c]pyrrole-1,4(2H,5H)-dione (**ClDPP**). As per the method described for **FDPP** using 4-chlorobenzonitrile (0.74 g, 5.4 mmol) and the pyrroline ester (0.9 g, 3.92 mmol) to give **ClDPP** as a bright red powder (0.85 g, 68 % yield).

3-(4-bromophenyl)-6-phenylpyrrolo[3,4-c]pyrrole-1,4(2H,5H)-dione (**BrDPP**). As per the method described for **FDPP** using 4-bromobenzonitrile (0.5 g, 2,7 mmol) and the pyrrolinecarboxylate ester (0.45 g, 1.96 mmol) to give **BrDPP** as a bright red powder (0.46 g, 65 % yield).

3-(4-iodophenyl)-6-phenylpyrrolo[3,4-c]pyrrole-1,4(2H,5H)-dione (**IDPP**). As per the method described for **FDPP** using 4-iodobenzonitrile (1.24 g, 5.4 mmol) and the pyrrolinecarboxylate ester (0.9 g, 3.92 mmol) to give **IDPP** as a bright red powder (1.22 g, 76 % yield).

2,5-dibenzyl-3-(4-fluorophenyl)-6-phenylpyrrolo[3,4-c]-1,4-(2H,5H)-dione (**FBDPP**). A suspension of **FDPP** (0.20 g, 0.65 mmol) and K_2CO_3 (1.05g, 0.65 mmol) in dry DMF (20 ml) was heated at 120 $^\circ$C under nitrogen atmosphere. At this temperature and under vigorous stirring, a benzyl bromide (1.92 ml, 16 mmol) solution in DMF (10 ml) was added over 20 minutes. Stirring and heating at 120 $^\circ$C were continued for 1.5 hours. After cooling to room temperature, salt was filtrated and washed with DMF. The remaining filtrate was collected and ice cold methanol/water was added to give an orange precipitate that was washed with water and then recrystallized from chloroform/hexane to afford **FBDPP** as an orange powder (0.14 g, 31 %). ^{1}H NMR (CDCl$_3$): 4.96 (2H, s, CH$_2$), 4.98 (2H, s, CH$_2$), 7.09-7.19 (5H, m, ArH), 7.24-7.32 (7H, m, ArH), 7.41-7.49 (3H, m, ArH) 7.73-7.78 (4H, m, ArH). ^{13}C NMR (CDCl$_3$): 45.70 (CH$_2$), 45.70 (CH$_2$), 116.18 (C=C), 116.39 (C=C), 124.14 (C=C), 124.17 (C=C), 126.66 (C=C), 126.77 (C=C), 127.51 (C=C), 127.58 (C=C), 127.87 (C=C), 128.89 (C=C), 128.97 (C=C), 129.13

(C=C), 131.48 (C=C), 131.56 (C=C), 137.40 (C=C), 137.47 (C=C), 147.94 (C=C), 149.20 (C=C), 162.78 (C=O), 162.86 (C=O). IR (ATR)/cm^{-1}: 3031 (ArH), 2943 (CH$_2$), 1654 (C=O), 1603 (C=C), 1495 (C=C), 821 (ArH), 736 (ArH), 690 (ArH). Anal. Calcd for C$_{32}$H$_{23}$FN$_2$O$_2$: C, 79.00; H, 4.76; N, 5.76. Found: C, 78.98; H, 4.84; N, 5.55. Melting point: 267-269 °C.

2,5-dibenzyl-3-(4-chlorophenyl)-6-phenylpyrrolo[3,4-c]-1,4-(2H,5H)-dione (**ClBDPP**). As per the method described for **FBDPP** using **ClDPP** (0.40 g, 1.23 mmol), K$_2$CO$_3$ (2.28 g, 1.23 mmol) and benzyl bromide (2.4 ml, 20 mmol) to give **ClBDPP** as an orange powder (0.51 g, 82 %). ^{1}H NMR (CDCl$_3$): 4.95 (2H, s, CH$_2$), 4.97 (2H, s, CH$_2$), 7.17-7.18 (4H, m, ArH), 7.23-7.32 (6H, m, ArH), 7.35-7.47 (5H, m, ArH) 7.68-7.70 (2H, d, ArH) 7.72-7.75 (2H, d, ArH). ^{13}C NMR (CDCl$_3$): 45.71 (CH$_2$), 45.71 (CH$_2$), 126.33 (C=C), 126.67 (C=C), 126.77 (C=C), 127.53 (C=C), 127.61 (C=C), 127.82 (C=C), 128.90 (C=C), 128.98 (C=C), 129.00 (C=C), 129.15 (C=C), 129.32 (C=C), 130.44 (C=C), 131.65 (C=C), 137.36 (C=C), 137.41 (C=C), 137.62 (C=C), 147.64 (C=C), 149.57 (C=C), 162.73 (C=O), 162.82 (C=O). IR (ATR)/cm^{-1}: 3030 (ArH), 2928 (CH$_2$), 1655 (C=O), 1601 (C=C), 1494 (C=C), 841 (ArH), 732 (ArH), 690 (ArH). Anal. Calcd for C$_{32}$H$_{23}$ClN$_2$O$_2$: C, 76.41; H, 4.61; N, 5.57. Found: C, 75.72; H, 4.88; N, 5.24. Melting point: 238-240 °C.

2,5-dibenzyl-3-(4-bromophenyl)-6-phenylpyrrolo[3,4-c]-1,4-(2H,5H)-dione (**BrBDPP**). As per the method described for **FBDPP** using **BrDPP** (0.30 g, 0.81 mmol), K$_2$CO$_3$ (1.5 g, 0.81 mmol) and benzyl bromide (2.4 ml, 20 mmol) to give **BrBDPP** as an orange powder (0.51 g, 82 %). ^{1}H NMR (CDCl$_3$): 4.95 (2H, s, CH$_2$), 4.97 (2H, s, CH$_2$), 7.17-7.18 (4H, d, ArH), 7.23-7.32 (6H, m, ArH), 7.41-7.49 (3H, m, ArH) 7.54-7.56 (2H, m, ArH), 7.60-7.62 (2H, m, ArH), 7.73-7.75 (2H, d, ArH). ^{13}C NMR (CDCl$_3$): 45.71 (CH$_2$), 45.71 (CH$_2$), 126.12 (C=C), 126.68 (C=C), 126.78 (C=C), 127.53 (C=C), 127.62 (C=C), 127.83 (C=C), 128.90 (C=C), 128.99 (C=C),

129.14 (C=C), 130.54 (C=C), 131.66 (C=C), 132.29 (C=C), 137.36 (C=C), 137.41 (C=C), 147.68 (C=C), 149.59 (C=C), 162. 71 (C=O), 162.82 (C=O). IR (ATR)/cm^{-1}: 3056 (ArH), 2943 (CH$_2$) 1673 (C=O), 1604 (C=C), 1493 (C=C), 828 (ArH), 730 (ArH), 689 (ArH). Anal. Calcd for C$_{32}$H$_{23}$BrN$_2$O$_2$: C, 70.21; H, 4.23; N, 5.12. Found: C, 70.25; H, 4.34; N, 4.99. Melting point: 235-236 °C.

2,5-dibenzyl-3-(4-iodophenyl)-6-phenylpyrrolo[3,4-c]-1,4-(2H,5H)-dione (**IBDPP**). As per the method described for **FBDPP** using **IDPP** (1.0 g, 2.4 mmol), K$_2$CO$_3$ (4.5 g, 2.4 mmol) and benzyl bromide (2.4 ml, 20 mmol) to give **IBDPP** as an orange powder (0.68 g, 47 %). ^{1}H NMR (CDCl$_3$): 4.94 (2H, s, CH$_2$), 4.97 (2H, s, CH$_2$), 7.16-7.18 (4H, m, ArH), 7.22-7.32 (6H, m, ArH), 7.41-7.49 (5H, m, ArH) 7.72-7.78 (4H, m, ArH). ^{13}C NMR (CDCl$_3$): 45.71 (CH$_2$), 45.71 (CH$_2$), 126.66 (C=C), 126.78 (C=C), 127.29 (C=C), 127.53 (C=C), 127.61 (C=C), 127.84 (C=C), 128.89 (C=C), 128.98 (C=C), 129.00 (C=C), 129.13 (C=C), 130.45 (C=C), 131.65 (C=C), 137.37 (C=C), 137.41 (C=C), 138.23 (C=C), 147.83 (C=C), 149.59 (C=C), 162.72 (C=O), 162.80 (C=O). IR (ATR)/cm^{-1}: 3031 (ArH), 2943 (CH$_2$), 1682 (C=O), 1592 (C=C), 1487 (C=C), 824 (ArH), 736, 691 (ArH). Anal. Calcd for C$_{32}$H$_{23}$IN$_2$O$_2$: C, 64.66; H, 3.90; N, 4.71. Found: C, 65.19; H, 3.96; N, 4.60. Melting point: 201-202 °C.

Preparation of Crystals for Single Crystal X-Ray Diffraction analysis. *FBDPP*: Slow evaporation of a cooled solution of **FBDPP** in hexane/chloroform (1:1). *ClBDPP*: Slow evaporation of a cooled solution of **ClBDPP** in hexane/chloroform (1:1). *BrBDPP*: Slow evaporation of a cooled solution of **BrBDPP** in hexane/chloroform (1:1). *IBDPP*: Slow evaporation of a cooled solution of **IBDPP** in hexane/chloroform (1:1).

Crystal structure determination. For *BrBDPP* data were measured at Station I19 of the DIAMOND synchrotron light source.[69] All other data were measured using laboratory based instruments and monochromated Mo radiation. All structures were refined to convergence, on F^2 and against all unique reflections with SHELX-97.[70] Highly disordered and partially present solvent was present in channels parallel to the *b* axis in both *BrBDPP* and *IBDPP*. As this could not be identified or modelled, the SQUEEZE routine of PLATON was implemented to remove the effects of approximately 58 electron equivalents from 221 Å^3 of unit cell space for *BrBDPP* and 56 electron equivalents from 247 Å^3 of unit cell space for *IBDPP*.[71] Table 1 summarises the different selected crystallographic data and refinement parameters for the crystal structures herein reported.

Table 1. Selected crystallographic data and refinement parameters for *XBDPP* compounds

Compound	FBDPP	ClBDPP	BrBDPP	IBDPP
Formula	$C_{32}H_{23}FN_2O_2$	$C_{32}H_{23}ClN_2O_2$	$C_{32}H_{23}BrN_2O_2$[a]	$C_{32}H_{23}IN_2O_2$[a]
Formula Weight	486.52	502.97	547.43[a]	594.42[a]
X-ray Source	micosource	microsource	synchrotron	rotating anode
Crystal system	Monoclinic	Monoclinic	Monoclinic	Monoclinic
Space Group	P 2₁/c	P 2₁/c	P 2₁/c	P 2₁/c
λ Å	0.71073	0.71073	0.6889	0.71075

a Å	12.7952(11)	13.0195(6)	22.15(4)	22.758(11)
b Å	15.4086(14)	15.3154(7)	5.300(8)	5.3375(19)
c Å	5.9945(5)	6.1283(3)	23.88(4)	24.226(11)
β°	97.086(5)	97.371(2)	115.082(17)	114.517(5)
Volume Å^3	1172.83(18)	1211.88(10)	2539(7)	2677(2)
Temp. K	123(2)	123(2)	100(2)	100(2)
Z	2	2	4	4
Refls. Collected	18254	21168	20642	15140
2θ max °	52.84	52.18	50.0	52.0
Refls. Unique	2407	2398	4831	5253
Refls. Obs.	1806	1946	3054	4069
Rint	0.0360	0.0282	0.1109	0.0641
Goodness of Fit	1.078	1.127	1.100	1.181
R[I>2s(I)], *F*	0.0404	0.0604	0.1057	0.0810
Rw, *F*^{2}	0.1030	0.1314	0.3123	0.1610
Max/min electron density eÅ^{-3}	0.149/-0.204	0.269/-0.428	0.868/-0.920	0.511/-0.711

Computational details. All molecular modelling studies were carried out using the Truhlar M06-2X density functional[72] and 6-311G(d) level as implemented in Spartan10 software.[73] This density functional has been shown to give good account of the dimer interaction energies of π-π interacting systems.[32,55] Dimer interaction energies, ΔE_{CP}, were all corrected for Basis Set Superposition Error (BSSE) using the counterpoise correction method of Boys and Bernardi.[74]

The computation of the dimer interactions of an **H₂DPP** model system were performed following the method previously described by us.[19] Herein, the triple zeta 6-311G(d) basis set was also employed for the model system and a comparison of these results with those previously reported employing a 6-31G(d) basis set was conducted. The halogen substitution effects on these systems were evaluated by means of two analogous model systems (denoted aligned and anti-aligned in line with previous nomenclature[56]) of a mono-substituted **BrDPP** system (which represents the non-benzylated analogue of **_BrBDPP_**) using the density functional M06-2X at 6-311G(d) level. Note the intermonomer separation (represented as Δz) for the **BrDPP** model system was set to Δz = 3.6 Å as optimised for the **H₂DPP** analogue by scanning the intermolecular distance at 0.3 Å increments while holding the monomers in a fully eclipsed relative orientation,[19] given that as extracted from halogen substituted crystal structures the presence of halogen atoms does not lead to any significant/systematic changes to the intermonomer distance along the z axis.

RESULTS AND DISCUSSION

Structural description. Structures of the di-halogenated species X_2BDPP (X = H, Cl, Br, I and B = N-benzyl) have been described by us previously.[19] They were found to form a structural series where, despite some slight, systematic variations, each compound displayed similar conformation and packing. An exception was one of the two observed polymorphs of Cl_2BDPP which differed from the others in terms of molecular conformation, packing and even colour. The four mono-substituted structures described here, $XBDPP$ (X = F, Cl, Br, I), fall into two structural groups with the fluoro- and chloro-derivatives being mutually isomorphous and isostructural and the bromo- and iodo-derivatives forming a second mutually isomorphous and isostructural pair. Interestingly, the F and Cl structures are also isomorphous with the "typical" polymorph of Cl_2BDPP, i.e. the polymorph that fits well into the X_2BDPP structural series. The X_2BDPP structures all contain crystallographically centrosymmetric molecules (Z' = 0.5) and despite the non-symmetrical mono-substitution of $FBDPP$ and $ClBDPP$ these structures also feature molecules that are situated at crystallographic centres of symmetry. The F and Cl atoms are thus disordered over two sites with 50 % occupancy. For $ClBDPP$ this structural approximation leads to somewhat elongated thermal displacement parameters as the reported C, N and O atom sites are in fact averages of two slightly different geometries. $FBDPP$ with a closer size match between X and H does not show the same distortions. The molecular conformations of $FBDPP$ and $ClBDPP$ are also in good agreement with the main conformation found for the X_2BDPP species. In all structures, the plane of the benzyl group ring approaches a perpendicular relationship with the DPP ring plane whilst the phenyl and halo-benzene rings are much less twisted with respect to the DPP ring plane (80.31(8) and 78.40(10); 23.18(16) and 24.25(17) ° for F and Cl species respectively). Presumably because of the increased geometrical

difference between H and X, the bromo- and iodo- structures do not feature crystallographically imposed molecular centrosymmetry, thus all four substituents are free to adopt their own conformations. Despite this, the conformation adopted is closely related to that seen for the fluoro-, chloro- and di-substituted analogues. The only difference is a slight increase in the degree of twist seen between the **DPP** plane and the planes of the conjoined aromatic rings (35.2(5) and 29.2(4) ° for the phenyl and halo-benzene rings of the bromo-derivative and 34.9(3) and 30.9(3) ° for the equivalent angles in the iodo-derivative; compare to a range of 20.6 to 24.3 ° for others).

Analysis of the intermolecular contacts of the four **XBDPP** species shows that all make three groups of contacts with intermolecular separations less than the sum of Van der Waals radii. These are π-π interactions, halo-π interactions and C-H…O/N hydrogen bonds. The latter are largely long range (H…O/N 2.35 to 2.58 Å) and relatively constant over the four structures and so will not be discussed further. The π-π stacking interactions are of particular interest with respect to optical-electronic properties and are found in each structure.
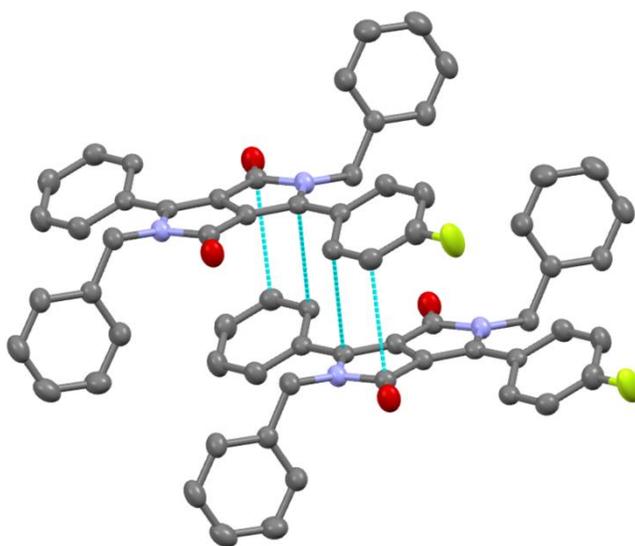
Figure 1. Short π-π contacts between a pair of ***FBDPP*** molecules assuming aligned orientation. The disordered F atom sites and all H atoms have been omitted for clarity.

For the fluoro- and chloro- derivatives, close interactions are found between the **DPP** ring system and the phenyl and/or halo-benzene rings, as illustrated in Figure 1. Note that the disorder in the X atom position makes it impossible to determine the relative orientation of the molecules in each pair. Each molecule makes interactions with two neighbouring molecules to give π-π stacks that propagate parallel to the *c* direction. The bromo- and iodo-derivatives make similar interactions and stacks, but it is apparent that short contacts involve only the **DPP** and phenyl rings (i.e. the halogenated rings are not involved) and as these are well ordered structures it can be seen that each close pair has a head to head orientation. In each pair, a second interaction between two benzyl group aromatic rings also occurs, illustrated in Figure 2.
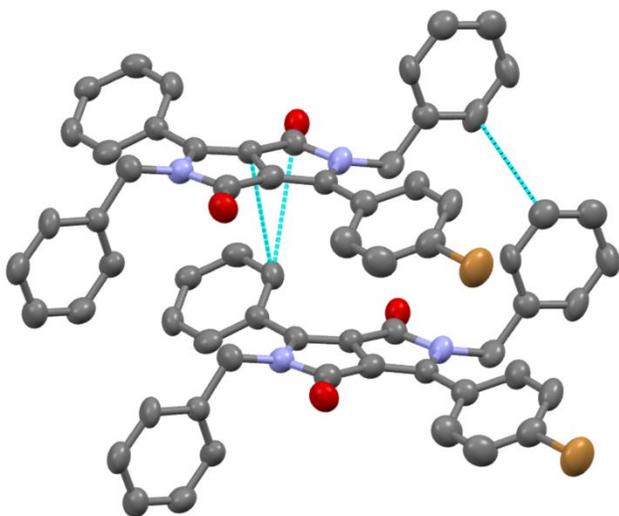
Figure 2. Short π-π contacts between a pair of **BrBDPP** molecules showing the observed aligned orientation. All H atoms have been omitted for clarity.

These interactions combine to give π-π stacks that propagate parallel to the crystallographic *b* direction. As with the fluoro- and chloro- species this is the short unit cell dimension. For the four **XBDPP** structures, the closest **DPP** to π C…C contacts are 3.290(2), 3.274(4), 3.357(11) and 3.453(8) Å for X = F, Cl, Br and I respectively. Thus, as well as making fewer such close contacts per molecule, the Br and I derivatives also make longer contacts. Indeed for **IBDPP** the shortest contact is longer than the sum of Van der Waals radii and the benzyl to benzyl π-π contact is shorter (3.380(10) Å) than the **DPP** to π contact. All four **XBDPP** structures make short halo-π contacts (shortest X…C 3.047(3), 3.086(4), 3.343(11) and 3.453(8) Å for X = F, Cl, Br and I respectively). For the Br and I structures these are X to benzyl interactions that link pairs of stacks whilst for the F and Cl structures these interactions also link stacks but now they do so by forming contacts between the non-benzyl benzene ring derivatives. The **BrBDPP** and **IBDPP** structures feature partially present solvent layers at approximately *a* = 0.5 and thus bilayers of **XBDPP** form parallel to the *bc* plane.

Intermolecular interaction energies, ΔE_{CP}. Given the crucial role played by π-π stacking motifs in determining the charge transfer properties of organic materials,[31,32,75] we devote the remainder of the paper to an in-depth investigation of substituent effects on the π-π dimer pairs of these systems. In order to widen our understanding of halogen substitution effects in DPPs as well as to further investigate head-to-head (aligned) versus head-to-tail (anti-aligned) relative intermonomer orientations with respect to the position of the halogen atoms, the intermolecular interactions, ΔE_{CP} for the π-π dimer pairs of the mono-halogenated **XBDPP** systems were

computed. The **FBDPP** and **ClBDPP** structures exhibit π-π dimer pairs which are stacked along the *c* crystallographic axis, analogous to the π-π dimer pair of their isomorphous "typical" polymorph of **Cl₂BDPP** (vide supra).[19] In turn, π-π dimer pairs of **BrBDPP** and **IBDPP** stack along the *b* crystallographic axis as opposed to their di-halogenated counterparts where the π-π dimer pairs were observed to stack along the *a* and *c* crystallographic axes for **Br₂BDPP** and **I₂BDPP** respectively.
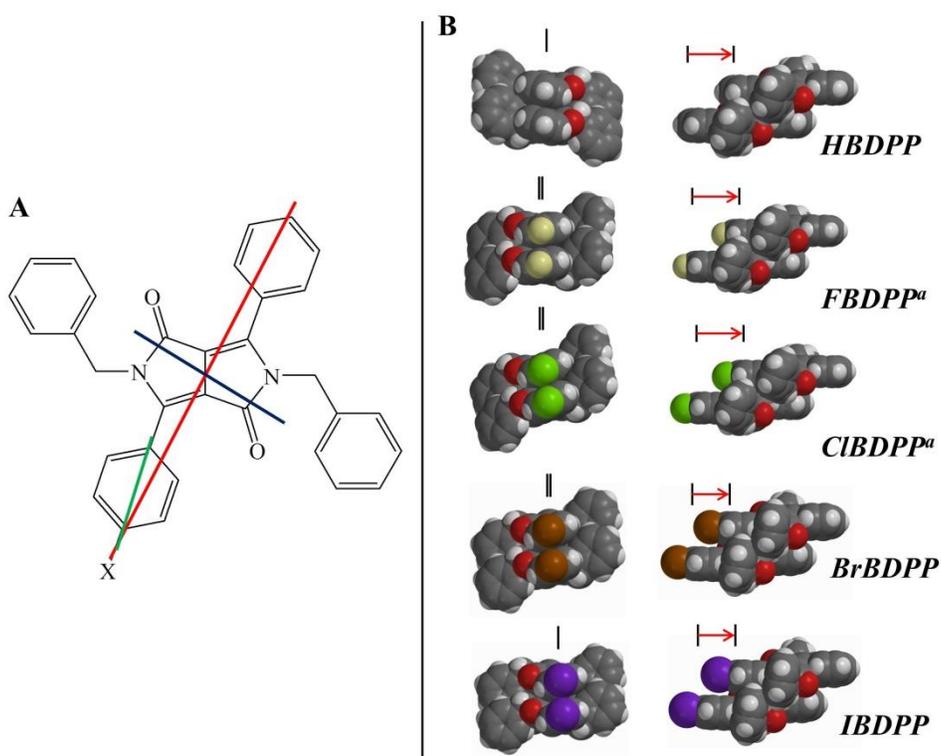

Figure 3. **XBDPP** crystal structures determined with short and long molecular axes in blue and red, respectively. Benzene axis denoted in green for comparison (**A**). Long (right) and short (left) molecular axis perspective views of the **HBDPP**,[19] **FBDPP**, **ClBDPP**, **BrBDPP** and **IBDPP** (**B**). [a]assuming aligned orientation.

Table 2. Intermonomer displacements exhibited by the π-π dimer pairs of *FBDPP*, *ClBDPP*, *BrBDPP* and *IBDPP*.

	FBDPP	*ClBDPP*	*BrBDPP*	*IBDPP*
Δx / Å	4.68	4.88	3.57	3.55
Δy / Å	0.20	0.30	0.23	0.05
Δz / Å	3.54	3.48	3.42	3.66

The π-π dimer pairs of *FBDPP*, *ClBDPP*, *BrBDPP* and *IBDPP* were observed to exhibit similar intermonomer displacements (see Table 2 for details). The relative alignment of monomers in each of the π-π dimer pairs appears to vary systematically according to the increased polarisability of the substituent on the para position of the phenyl rings attached to the central core, with *IBDPP* displaying the smallest degree of long molecular axis slip (see Figure 3). Significant differences were observed in the displacements of the π-π dimer pairs of *BrBDPP* and *IBDPP* systems along their long molecular axes compared to the di-halogenated equivalents (Δx = 8.44 and 9.40 Å for *Br₂BDPP* and *I₂BDPP* respectively), whereas Δy shift measured for *ClBDPP* was more in line with the equivalent di-halogenated system, *Cl₂BDPP* (Δx = 5.13 Å). Displacements along the short molecular axis were observed to be in line with those exhibited by other N-benzyl substituted DPP systems.[19,20] Accordingly, these systems reinforce the importance of N-substitution in crystalline DPPs over and above a recognised solubilising effect. Similarly to the di-halogenated symmetrical analogues, in asymmetric halogenated N-substituted DPPs the presence of benzyl groups on the lactam nitrogen definitively preclude any significant

displacement along the short molecular axis, which is in sharp contrast to the non N-substituted pigmentary equivalents such as **H₂DPP**, **Cl₂DPP** and **diphenylDPP** for which 1.8 Å < Δy < 5.6 Å.[27-29]
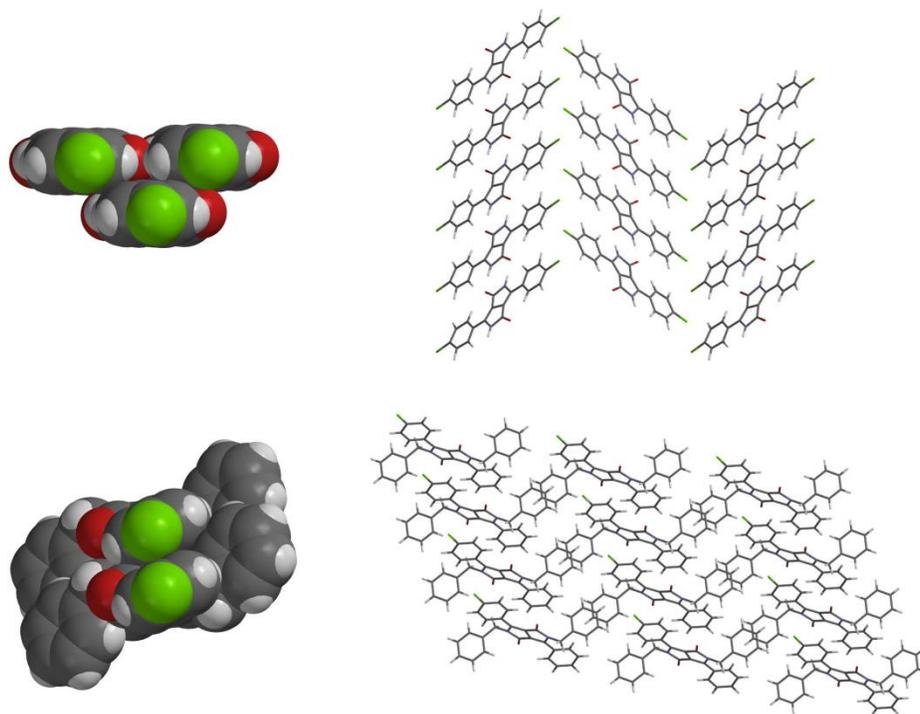

Figure 4. Illustration of Δy shifts in the π-π dimer pairs (left) and herringbone vs slipped cofacial packing motifs (right) of **ClDPP** (top) and **ClBDPP** (bottom) respectively.

An additional effect of N-benzylation is in the disruption of the herringbone structure, which is characteristic of DPP pigments, to a slipped stack as illustrated in Figure 4 for **ClDPP** and **ClBDPP**. N-substituted DPP crystal structures have been previously reported[21] employing alkyl chain solubilising groups instead of benzyl substituents. The measured displacement (Δy = 1.80 Å) of the monomers in the π-π stack of the latter were observed to be more in line with the pigment analogues and to exceed that of the N-benzyl counterparts. Thus, our previous studies,

and those structures reported herein highlight the important role played by benzyl groups in facilitating the design of crystalline DPP systems which maximise spatial and hence wavefunction overlap, widely recognised as being critical in the optimisation of effective charge transport behaviour. [19,26,31,33]

We initially investigated the position of the halogen atoms in the disordered structures of **FBDPP** and **ClBDPP** (vide supra) as well as the role of benzyl stabilisation of these π-π dimer pairs (see Figure 5 for details). Intermolecular interaction energies were computed for the different dimer pairs possible (where dimer pairs A, B and C denote the relative position of the halogen atom in the bottom and top monomer as in-in, in-out and out-out respectively, as illustrated in Figure 5) from the disordered model and from these the role of benzyl, halogen and simultaneous benzyl/halogen substitution was rationalised through a series of systematically cropped dimer pairs. In short, the benzyl (B) and halogen (X) substituents were removed and replaced with H atoms, first individually, and then simultaneously, resulting in **XDPP**, **BDPP**, and **DPP** structures respectively, where **XBDPP** denotes the uncropped dimer pair. Table 3 summarises the computed ΔE_{CP} for these systems.

Table 3. Counterpoise corrected intermolecular interactions energies, ΔE_{CP} for a series of structurally modified and non-structurally modified π-π dimer pairs of **FBDPP/ClBDPP**.

Dimer pair	ΔE_{CP} / KJ mol^{-1}			
	XBDPP	XDPP	BDPP	DPP
A	-62.35/-72.54	-39.09/-49.23	-63.06/-63.75	-39.90/-40.55

B	-63.58/-67.05	-40.10/-44.86	-63.06/-63.75	-39.90/-40.55
C	-63.80/-61.44	-39.92/-39.84	-63.06/-63.75	-39.90/-40.55

The π-π dimer pairs of *FBDPP* exhibit negligible (< 1 kJ mol^{-1}) fluorine induced stabilisation as extracted from the computed intermolecular interaction energies arising for the examined dimer pairs. This finding is consistent with the absence of any intermolecular short contact interactions involving fluorine atoms and the low polarisability of C-F bonds.[76,77] Consequently, none of these dimer pairs is significantly more energetically favoured in relation to the position of the halogen atoms. Benzyl induced stabilisation can be identified via comparison of the **BDPP** and **DPP** cropped dimer pairs. In line with other DPP systems characterised by similar intermonomer displacements,[19] benzyl induced stabilisation in this case arises from the additive contribution of slipped cofacial interactions[57,59] between the benzylic phenyl rings, a so-called T-shape interaction[42,52] between the benzylic phenyl rings and the phenyl rings attached to the central core and an attractive H-bonding interaction between the electronegative carbonyl oxygen and the electropositive methylene hydrogens, which are separated by 3.082 Å. Analogous benzyl induced stabilisation was computed for the various dimer pairs of *ClBDPP*, which is consistent with similar intermonomer displacements along the short and long molecular axes compared to the fluorinated equivalent.
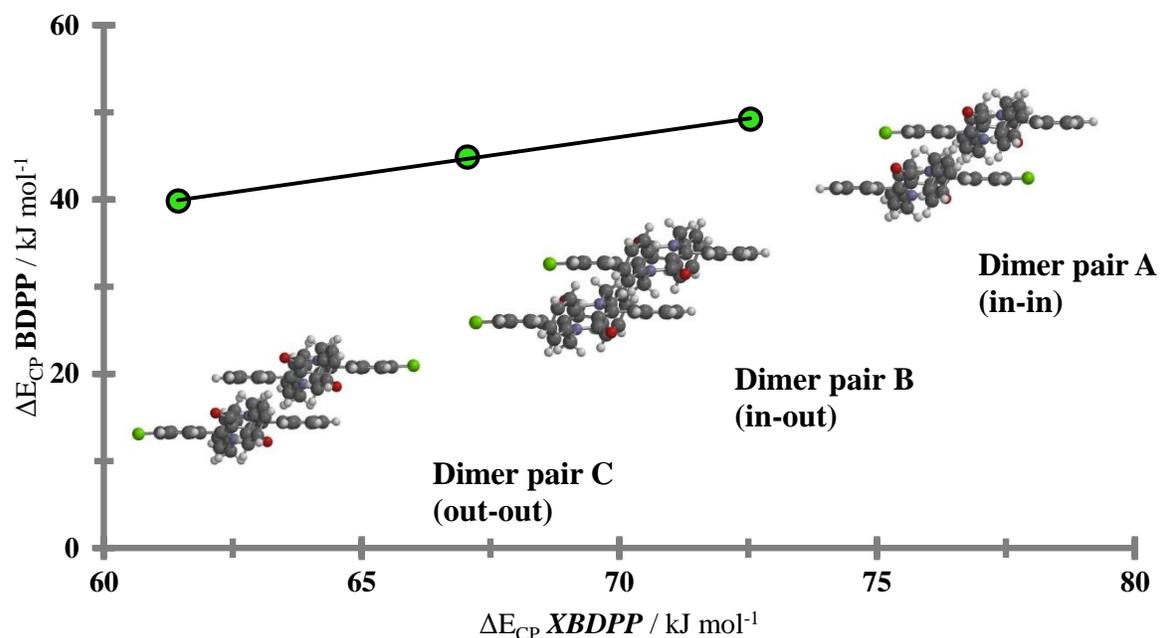
Figure 5. Computed ΔE_{CP} for **XDPP** vs *XBDPP* dimer pairs of *ClBDPP*. Inset illustrates different π-π dimer orientations investigated.

Unlike its fluorinated equivalent, computed intermolecular interactions for the various π-π dimer pairs of *ClBDPP* were observed to be influenced by the relative dimer orientation. In this regard, dimer pair A (in-in) was computed to be the most stable as a result of halogen induced stabilisation (ΔE_{CP} = -72.54, -67.05 and -61.44 kJ mol^{-1} for dimer pairs A, B and C of *ClBDPP* respectively), arising solely from dipole/induce dipole attractive intermolecular interactions between the C-Cl bond and the C-C linking the phenyl rings to the central DPP core. In this case no significant halogen-benzyl induced stabilisation was observed. Figure 5 illustrates the linear relationship (r^2 = 0.999) exhibited by computed ΔE_{CP} for *XBDPP* and **XDPP** for the various orientated dimers of *ClBDPP*. It is worthwhile to note that the role of halogen substitution is additive in these systems, as observed from plots of computed ΔE_{CP} for *XBDPP* and **XDPP** versus number of halogen atoms in the dimer pair (r^2 = 1.000 and 0.998 respectively), which is

consistent with current theories describing the role of halogen atoms involved in non-covalent interactions.[52,53,56,58,60]

Intermolecular interaction energies were also computed for the crystallographically observed π-π dimer pairs of **BrBDPP** and **IBDPP** and the role of benzyl/halogen in stabilising these dimer pairs was investigated analogously to the fluorinated and chlorinated derivatives (vide supra). Table 4 summarises the computed intermolecular interactions for **BrBDPP** and **IBDPP**.

Table 4. Counterpoise corrected intermolecular interactions energies, ΔE_{CP} for a series of structurally modified and non-structurally modified π-π dimer pairs of **BrBDPP** and **IBDPP**.

Compound	ΔE_{CP} / KJ mol^{-1}			
	XBDPP	XDPP	BDPP	DPP
BrBDPP	-79.16	-44.51	-76.45	-41.90
IBDPP	-79.36	-45.40	-76.81	-41.25

Intermolecular interactions, ΔE_{CP} of -79.16 and -79.36 kJ mol^{-1} were computed for the π-π dimer pairs of **BrBDPP** and **IBDPP** respectively. These almost identical values of ΔE_{CP} are consistent with the very subtle structural effects on progression from Br to I substituted N-benzyl DPPs such as the torsion of the ring bearing the halogen substituent with respect to the phenyl core (29.90 and 29.44° for **BrBDPP** and **IBDPP** respectively) and the intermonomeric displacement along the long molecular axis (vide supra). The intermolecular interactions exceed in all cases

those computed for the π-π dimer pair of Rubrene (-35.60 kJ mol^{-1}, M06-2X/6-311G(d)). Thus,

we propose, in line with our previous report[18], a greater thermal integrity of mono-halogenated

DPP single crystals compared with Rubrene; a very desirable property given the high sensitivity

of the charge transfer integrals for both hole and electrons (t_h and t_e respectively) to very small

intermolecular displacements.[19,26,31,33] In both π-π dimer pairs, the contribution of the halogen

atoms to the total intermolecular interactions is identified via comparison of *XBDPP* with **BDPP**

and **XDPP** with **DPP**. In each case, the action of cropping the halogen atoms from both

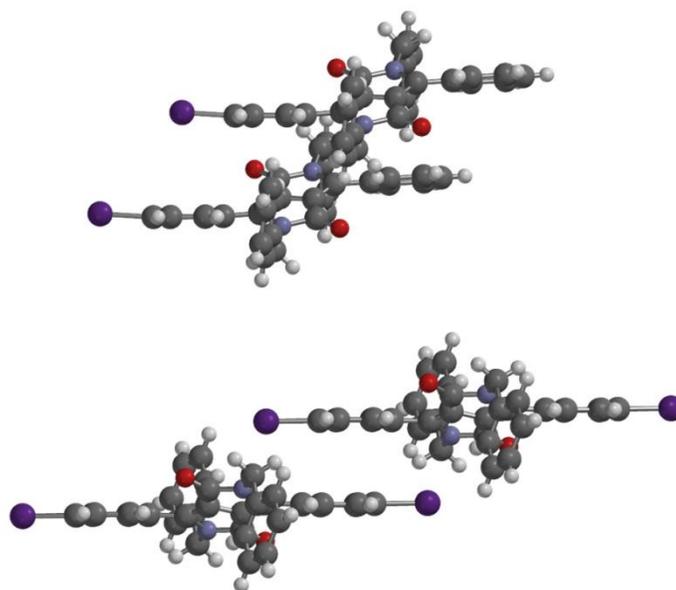monomers results in very small, ca 2-4 kJ mol^{-1} destabilisation of the dimer pair interaction

energy.

Figure 6. π-π dimer pairs of *IBDPP* (top) and *I₂BDPP*[19] (bottom) illustrating the intermonomer

contacts for their significantly different slips along the long molecular axis.

Of note is the small destabilisation computed on progression from *XBDPP* to **BDPP** (2.71 and

2.55 kJ mol^{-1} for *BrBDPP* and *IBDPP* respectively) which contrasts to the computed values for

analogous dimer pairs of the di-halogenated equivalents (16.1 and 23.49 kJ mol^{-1} for ***Br₂BDPP***

and ***I₂BDPP*** respectively).[19] This can be readily explained through analysis of the different

displacements exhibited by mono and di-halogenated π-π dimer pairs along their long molecular

axis (vide supra) as illustrated in Figure 6. In short, the computed destabilisation observed on

cropping the halogen atoms in the di-halogenated systems arises from close intermolecular

electrostatic interactions between the electropositive phenylic hydrogens and the electronegative

halogen atoms, which in ***BrBDPP*** and ***IBDPP*** are precluded given the shorter dimer

displacements along the long molecular axis. In turn, the role of the benzyl substituents in

stabilising these π-π dimer pairs can be understood from the comparison of ***XBDPP*** with **XDPP**

and **BDPP** with **DPP**. In light of the very small halogen contribution to ΔE_{CP}, the effect of

cropping the benzyl groups should be similar by comparing both pairs. In fact, variations in

intermolecular interactions of 34.65/34.55 and 33.96/35.56 kJ mol^{-1} were computed for ***XBDPP***

vs. **XDPP** and **BDPP** vs. **DPP** for ***BrBDPP*** and ***IBDPP*** respectively. The large benzyl

stabilisation of these π-π dimer pairs was identified to arise from three different contributions: a

slipped phenyl-phenyl type between the two phenyl rings within the benzyl groups,[57,59] a

T-shaped interactions between the benzylic phenyl rings and the phenyl rings attached to the core

of the DPP[42,54] and a third electrostatic contribution arising from the close contact between the

electronegative carbonyl oxygen of one monomer and the electropositive methylene/phenylic

hydrogen atoms of the other monomer. The importance of N-benzyl substitution, over and above

a solubilising effect and steric influence on precluding significant shifts along the short

molecular axis, is therefore clearly exhibited by an enhancement of the stabilisation of these π-π

dimer pairs. This finding is in contrast with previous reports of DPP systems which employ

alkyl chain as N-substituents.[21]

Given our interest in developing charge transfer mediating materials based on N-substituted DPPs, we calculated the hole (t_h) and electron (t_e) transfer integrals for the π-π dimer pairs of **BrBDPP** and **IBDPP** by means of an **H₂DPP** model system (vide infra and SI2) since both of these dimer pairs exhibit negligible intermonomer displacement along the short molecular axis. We propose on the basis of the calculated integrals that both π-π dimer pairs of **BrBDPP** and **IBDPP** should be characterised by larger electron than hole transfer (t_h = 2.84 and t_e = 14.13 kJ mol^{-1} at Δx = 3.6 Å, SI2) in light of their displacement along the long molecular axis.

In conclusion, we find that removal of the benzyl groups on progression from **BDPP** to **DPP** results in decreasing the ΔE_{CP} (-79.16 and -79.36 kJ mol^{-1} for **BrBDPP** and **IBDPP** respectively) by 43.65 and 44.81 % for **BrBDPP** and **IBDPP** respectively. In turn, removal of the bromine/iodine atoms on progressing from **XDPP** to **DPP** results in a destabilisation of the total ΔE_{CP} by 3.30 % for **BrBDPP** and 5.23 % for **IBDPP**. Systematic halogen substitution in DPPs therefore appears to play an important role in defining the intermonomer displacements along the long molecular axis, which facilitate determination of intermolecular interactions and associated charge transfer integrals in these systems.[19] Accordingly, we dedicate the remainder of the paper to an in-depth investigation of halogen substitution in DPP structures of this type through analysis of a series of novel model dimer systems.

Dimer model system. We have previously reported a DPP model system formed by two non-substituted **H₂DPP** monomers where the top monomer is shifted with respect to the bottom one from a fully eclipsed geometry through the long molecular axis across a distance of 15.3 Å in 0.3 Å increments while retaining Δy = 0.00 Å and Δz = 3.60 Å. Herein, we revisit this model system employing an enhanced triple zeta basis set and the analogies in the computed data are briefly discussed. It is of interest that π-π dimer pairs of **FBDPP** and **ClBDPP** are characterised

by shifts (Δx = 4.68 and 4.88 Å respectively) closely related to the local minima at ca 5.1 Å and that those of **BrBDPP** and **IBDPP** exhibit displacements along their long molecular axes (Δx = 3.57 and 3.55 Å respectively) coinciding with the global minimum predicted by the potential energy surface (PES) of the model system. It is also of particular interest that both monomers in the dimer pairs of **BrBDPP** and **IBDPP** are aligned with respect to the relative orientation of the halogen atoms. In this regard, we report two additional model systems and compute their interaction energies as a function of long molecular axis dimer displacement, where the relative orientation of the halogen atoms on each monomer is aligned and anti-aligned with respect to one other.
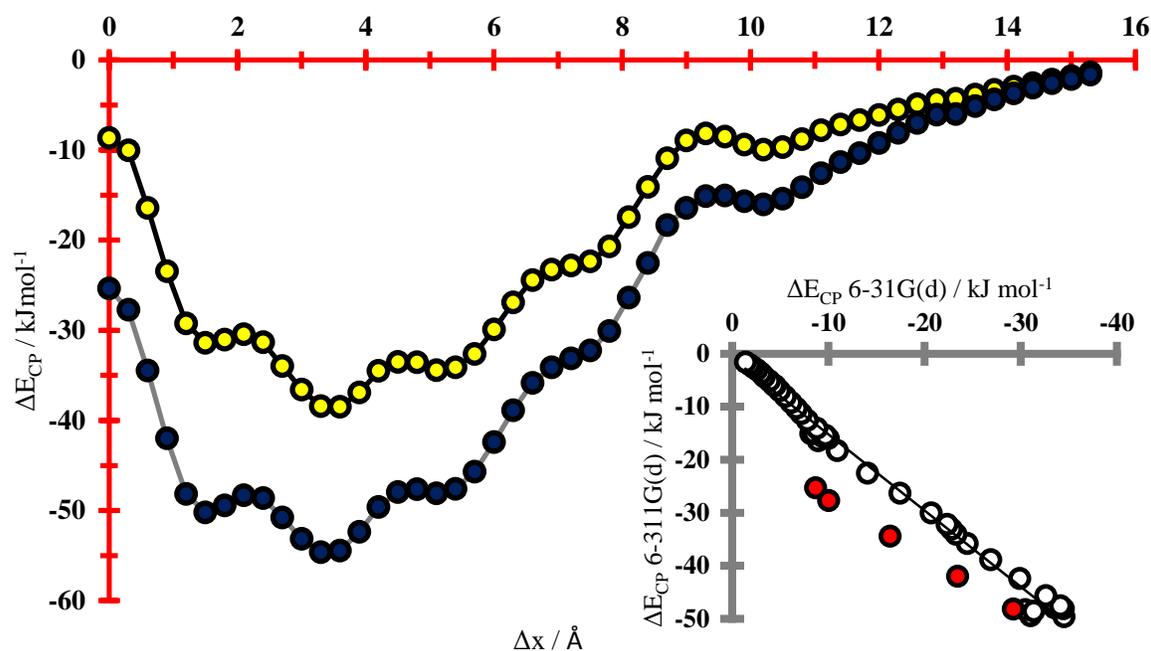

Figure 7. Counterpoise corrected **H₂DPP** model dimer interaction energy as a function of intermonomer slip (Δx) at M06-2X/6-31(d) (yellow filled circles) and M06-2X/6-311G(d) (blue filled circles). Inset illustrates linear regression between computed ΔE_{CP} for 6-31G(d) and 6-311G(d) with red filled circles representing the dimer pairs with $\Delta x \leq 1.2$ Å.

Figure 7 illustrates the computed PES for the **H₂DPP** model system determined using double and triple zeta basis sets. Significantly greater intermolecular interactions energies (ΔE_{CP} = -38.52 and -54.46 kJ mol^{-1} for 6-31G(d) and 6-311G(d) respectively at Δx = 3.6 Å) were computed throughout the entire studied range of displacements along the long molecular axis by means of the triple zeta basis set. The inset in Figure 7 illustrates the relationship between the computed ΔE_{CP} by means of the two employed basis sets. Both potential energy surfaces denote the same number of inflections located at identical shifts along the long molecular axis. However, the inset in Figure 7 illustrates that the linear relationship (r^2 = 0.992) exhibited between computed ΔE_{CP} by means of 6-31G(d) and 6-311G(d) is diminished for dimer pairs characterised by $\Delta x \leq 1.2$ Å (denoted by red filled circles in the inset in Figure 7). In order to further investigate this finding, we reproduced our previous cropped dimer model[19] at the 6-311G(d) level of theory (SI1); where we previously reported repulsive interaction energies for fully eclipsed/quasi-eclipsed ($\Delta x \leq 0.6$ Å) phenyl-phenyl (ΔE_{CP} = 3.07 kJ mol^{-1} at Δx = 0.00 Å) interactions using a 6-31G(d) basis set. Contrary to our previous findings and to common chemical intuition, attractive intermolecular interaction energies were computed for these cropped dimer pairs (ΔE_{CP} = -3.05 kJ mol^{-1} at Δx = 0.00 Å) by means of the wider 6-311G(d) basis set. In fact, this is consistent with current studies on charge penetration effects at interplanar distances lower than 4 Å reported by Sherrill and co-workers,[53] given that at such intermonomeric distances the electron clouds do not repel each other as much as point charges do, since intermolecular electron-nuclear attractive term becomes larger than the sum of the electron-electron and nucleus-nucleus repulsive contributions. Accordingly, in the following all of the reported model dimer systems were computed by means of the M06-2X density functional at 6-311G(d) level. Along these lines, we observed the location

of the global minimum at ca. 3.6 Å in our computed potential energy surfaces to be independent of the basis set employed in the calculation.

The nature of interactions responsible for the stability in perfectly co-facial π-π dimer systems such as those investigated herein has been a matter of extensive debate in recent years.[34,35,38-60,65,78-80] The often employed description based on donor-acceptor interactions postulated by Hunter and Sanders (π-resonance-based model)[34,35,38,39] and the π/polar model of Cozzi and Siegel[65,80] have been shown to inadequately describe these types of interactions since they neglect the crucial role played by dispersion effects. Subsequent studies reported by Wheeler and Houk[48,49,55,60] as well as Sherrill and co-workers[41-44,52-54] have proven that π-π dimer pairs are instead stabilised by local bond dipole/bond dipole and bond dipole induced interactions leading to slipped co-facial interactions. Our results are in line with these more recent treatments of intermolecular π-π interactions. In order to broaden our understanding of the intermolecular interactions in crystalline mono-halogenated DPPs and to explore in detail the role of these interactions in stabilising the extracted crystal dimer pairs, the model dimer systems, including those aligned and anti-aligned pairs were cropped into a series of smaller dimers where the phenyl rings on either side of the DPP central core were denoted as A(A') and C(C') with the DPP core represented by B(B'). The notation X/X' indicates the units from the top and bottom monomers in the dimer pair respectively, as illustrated in Figure 8.
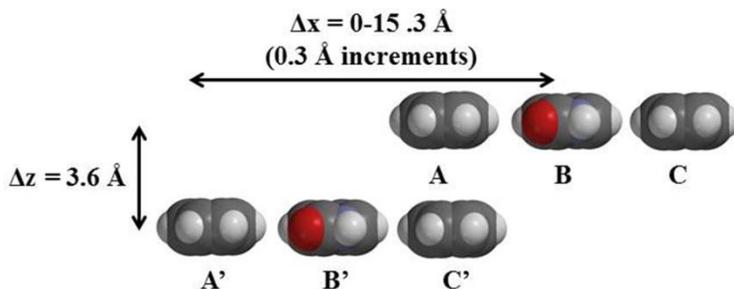
$\Delta x = 0\text{-}15.3\ \text{Å}$
(0.3 Å increments)

$\Delta z = 3.6\ \text{Å}$

A   B   C

A'   B'   C'

Figure 8. Illustration of the fragmented **H₂DPP** dimer pair employed in the model system.

Note, that in the case of the aligned **BrDPP** dimer model (non-benzylated analogue of ***BrBDPP***) both A and A' units bear a bromine atom. In turn in the anti-aligned model, A and C' are represented by bromobenzene units. Accordingly, each model system represented in Figure 8 was broken up into nine different components with a varying number of energetically equivalent X-X' dimer pairs for each model system (i.e. A-A' = C-C', B-A' = C-B' and A-B' = B-C' in the **H₂DPP** model system).[19]
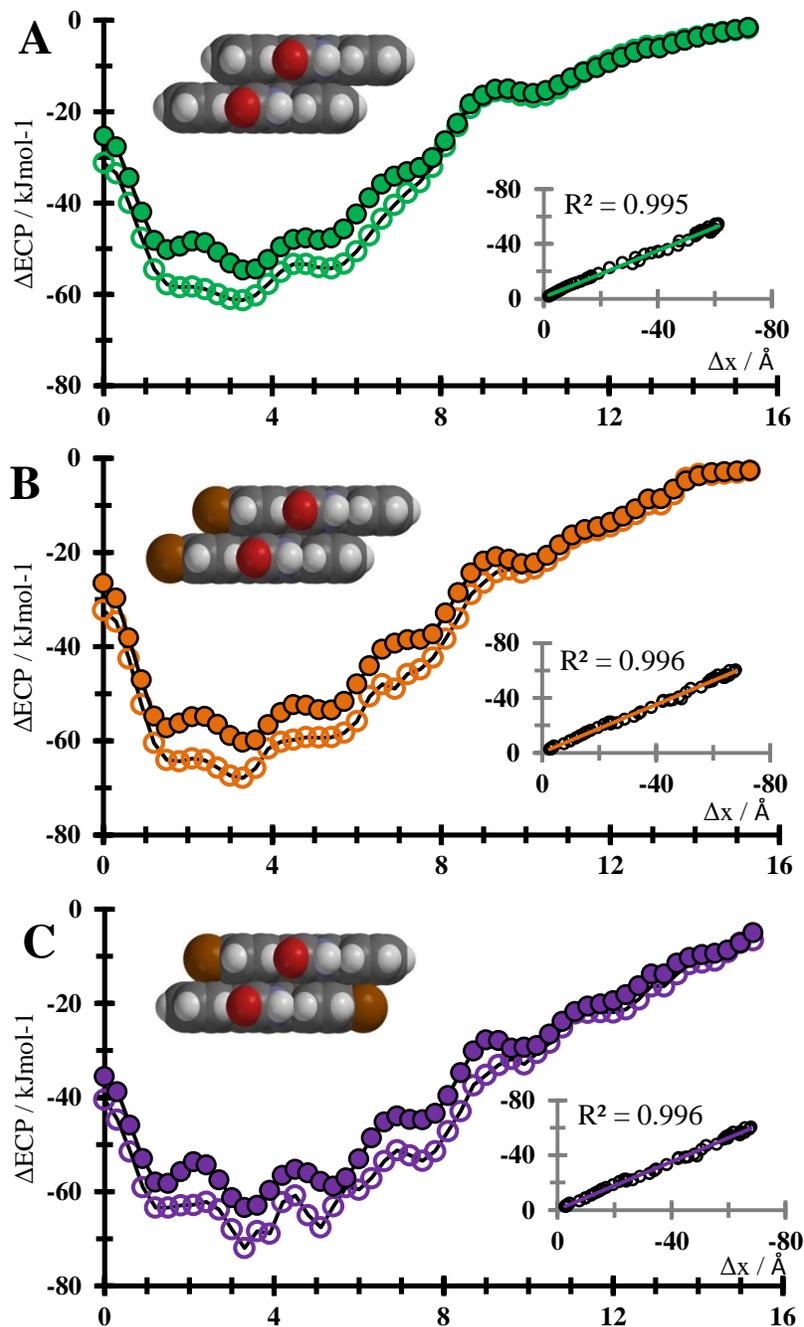
Figure 9. Counterpoise-corrected M06-2X/6-311G(d) **H_2DPP** (A), aligned **Br_2DPP** (B) and anti-aligned **Br_2DPP** (C) model dimer interaction energy as a function of intermonomer slip, Δx. Non-filled circles denote intermolecular interactions as a sum of the parts. Inset depicts linear regression of ΔE_{CP} (kJ mol^{-1}) computed for uncropped dimer system vs. associated values for the

sum of the parts of cropped model. Illustrated dimers correspond to energy minimum at $\Delta x = 3.6$ Å).

Figure 9 illustrates the computed PES for the model dimer of **H₂DPP** (A), the aligned dimer of **BrDPP** (B) and the anti-aligned dimer of **BrDPP** (C). Each of the model dimer systems are characterised by the same number of inflections in their potential energy surfaces, with minima located at identical shifts along the long molecular axis (ca $\Delta x = 1.5, 3.5, 5.1, 7.5$ and 10.2 Å), with the global minimum located at ca 3.5 Å. Accordingly, the PES for aligned and anti-aligned **BrDPP** model systems also predict the possibility of polymorphism in crystal structures of mono-halogenated DPPs, which is similar to our previous observation with the di-halogenated equivalents.[19] It is of note that both of the crystal extracted π-π dimer pairs of *BrBDPP* and *IBDPP* exhibit negligible displacements along their short molecular axes and a shift along the long molecular axis which is coincidental to the global minimum predicted by the model system (3.57 and 3.55 Å for *BrBDPP* and *IBDPP* respectively). In addition, the PES computed as the sum of the parts is consistently lower in energy compared to the PES for the uncropped dimer pairs. As reported by us previously,[19] this is consistent with the additional number of C-H bonds formed upon cropping of the respective monomers, hence increasing the number of local bond dipole and induced bond dipole interactions in these systems. In fact, a plot of the computed ΔE_{CP} for the cropped versus uncropped dimer models was observed to be linear in each of the reported model dimer systems (see insets in Figure 9, $r^2 = 0.995, 0.996$ and 0.996 for **H₂DPP**, aligned **BrDPP** and anti-aligned **BrDPP** dimer model respectively). If stabilisation of the dimer pairs arises from charge transfer interactions deriving from their respective HOMO/LUMO

π-orbitals, then the scenario illustrated by the PES reported in Figure 9 would not be expected, since these orbitals are broken up during cropping of the individual monomer units.

Via analysis of the cropped model systems, we identified, based upon their lower interaction energies, dimer pairs A-A' (phenyl/phenyl), A-B' (phenyl/DPP) and A-C' (phenyl/phenyl) as those which were required to account for the differences illustrated in Figure 9 upon halogen substitution, A summary of the key dimer intermolecular interactions in each of these systems is highlighted below, with a detailed analysis presented in SI 3-4.

Whereas in our previous report,[19] where cropped dimer pairs were primarily stabilised by means of dispersion forces, introduction of halogen atoms denotes an additional important electrostatic contribution that can outweigh these dispersion effects.[42,53,81] For global minima conformations of A-A' and A-C', coinciding with the top monomer (A) being located midway along then length of the benzene ring of the bottom monomer (A' and C' respectively), computed trends in binding energies were observed to be consistent with previous studies.[41,82] Interestingly, the computed intermolecular interaction (ΔE_{CP} = -9.86 kJ mol^{-1}) for the most stable configuration of the benzene/benzene dimer was observed to be slightly lower than that reported employing symmetry-adapted perturbation theory (ΔE_{CP} = -11.29 kJ mol^{-1})[41,82] which we attribute to the 12.76° offset in the long molecular axis of **H$_2$DPP** with respect to that of the benzene monomer (see Figure 3). Of note is the apparent additive effect observed upon halogenation for the different A-C' dimer pairs, which is in agreement with previous studies for fully eclipsed and slipped interactions, where an additive effect of the substituents was reported, as long as these were not within each other's local environment.[52,53,56,58,60] Benzene/DPP and bromobenzene/DPP (dimer pairs A-B' in the cropped model system) represent a major contribution to the computed PES illustrated in Figure 9, with computed global and local minima at ca 5.4 and 3.6 Å

respectively. Greater stabilisation of the A-B' dimer at the global minimum was observed upon bromination than that at the local minimum at ca 3.6 Å, attributed to an enhanced role played by the bromine atom in stabilising this dimer pair at $\Delta x = 5.4$ Å, given the closer intermolecular contacts.

Based on those interactions described above (and in SI 3-4), we believe that our analysis of the proposed model DPP systems demonstrate that the π-resonance model[34,35,38,39] is inadequate to represent non-covalent intermolecular interactions in crystalline halogenated DPPs and that our results are in line with the current description of π-π interactions.[41-44,48,49,52-55,60] The larger stabilisation energies computed for aligned and anti-aligned **BrDPP** dimer pairs is attributed to more favourable electrostatic interactions obtained via halogen substitution, which outweigh the predominantly dispersion effects observed in **H₂DPP** dimer pairs. Whilst the larger computed stabilisation energies for the anti-aligned compared with aligned **BrDPP** model system does not account for the observed aligned relative orientation of the halogen atoms in the crystal extracted π-π dimer pairs of **BrBDPP** and **IBDPP** we attribute the relative orientation of these dimers to be controlled by more favourable intermolecular interactions with other nearest neighbour dimer pairs.

CONCLUSIONS

In conclusion, four novel, and structurally related mono-halogenated N-benzyl substituted DPPs and their respective single crystal structures are reported. Crystal packing motifs for all of the studied structures exhibit π-π stacking motifs running the length of the crystal with small ($\Delta y < 0.30$ Å) intermonomer displacements along their short molecular axes arising through N-benzyl substitution. Displacements along the long molecular axis for each of the π-π dimer

pairs are coincident with those predicted by computed model systems, with the observed closer alignment for the **BrBDPP** and **IBDPP** π-π dimer pairs attributed to their greater polarisability. Crystallographic analysis reveals disordered structures of **FBDPP** and **ClBDPP** in relation to the position of the halogen atoms on each monomer. We compute the π-π dimer pair A (in-in) of **ClBDPP** to be more energetically favoured whereas negligible fluorine induced stabilisation was computed for any π-π dimer pair of **FBDPP**. The π-π dimer pairs of **FBDPP** and **ClBDPP** exhibit significant benzyl induced stabilisation. We also find that the computed intermolecular interactions of **BrBDPP** and **IBDPP** π-π dimer pairs are primarily stabilised via benzyl substitution (43.65 and 44.81 % of total ΔE_{CP}) and that the halogen atoms are only responsible for a small contribution (3.30 and 5.23 % of the total ΔE_{CP}). The effects of halogen substitution on the energetics of the intermolecular interactions between aligned and anti-aligned cofacial non-substituted DPP based dimer pairs were investigated, employing associated model systems by means of the M06-2X density functional at 6-311G(d). We find that a triple zeta basis set is superior to the previously employed 6-31G(d) basis set, in accounting for charge penetration effects at the investigated dimer interplanar distance. Importantly, the associated PES for each of these model systems exhibit the same number of inflections located at identical shifts along the long molecular axis shift (Δx). The greater stabilisation of halogen substituted DPP systems compared with their non-substituted equivalents is attributed to electrostatic effects outweighing stabilisation via dispersion in the non-halogenated **H₂DPP** dimer. We have therefore shown through these model systems that intermolecular interactions in halogenated DPP systems are inadequately represented by the π-resonance and π/polar models and in turn are more consistent with current theories that associate stabilisation to local bond dipole/bond dipole and bond dipole induced interactions. We hope the data reported herein is of value to those engaged in tuning

intermolecular interactions in π-conjugated systems and in particular to the design of novel crystalline DPP architectures via judicious application of supramolecular synthons.

SUPPORTING INFORMATION

Computed intermolecular interactions and associated charge transfer integrals for the **H₂DPP** dimer model system at M06-2X/6-311G(d). Computed intermolecular interactions for aligned and anti-aligned **ClDPP** and **BrDPP** dimer model systems and cropped dimer model system of **BrDPP** at M06-2X/6-311G(d). X-ray crystallographic information files (CIF) are available free of charge via the Internet at http://pubs.acs.org. Crystallographic information files are also available from the Cambridge Crystallographic Data Centre (CCDC) upon request (http://www.ccdc.ca.ac.uk); CCDC deposition numbers 1429262-1429265.

AUTHOR INFORMATION

Corresponding Authors

*E-mail: callum.mchugh@uws.ac.uk

*E-mail: jesus.calvo@uws.ac.uk

Notes

The authors declare no competing financial interest.

ACKNOWLEDGMENTS

REFERENCES

(1)   Smith, H. M. *High Performance Pigments*; Wiley-VCH, 2002.

(2)   Hao, Z. M.; Iqbal, A. *Chem. Soc. Rev.* **1997**, *26*, 203.

(3)   Christie, R. M. *Colour Chemistry*; The Royal Society of Chemistry, 2001.

(4)   Herbst, W.; Hunger, K. *Industrial Organic Pigments*; Wiley-VCH, 2004.

(5)   Wallquist, O.; Lenz, R. *Macromolecular Symposia* **2002**, *187*, 617.

(6)   Liu, J.; Sun, Y.; Moonsin, P.; Kuik, M.; Proctor, C. M.; Lin, J.; Hsu, B. B.; Promarak, V.; Heeger, A. J.; Thuc-Quyen, N. *Adv. Mater.* **2013**, *25*, 5898.

(7)   Hong, W.; Sun, B.; Aziz, H.; Park, W.-T.; Noh, Y.-Y.; Li, Y. *Chem. Commun.* **2012**, *48*, 8413.

(8)   Lee, J.; Cho, S.; Seo, J. H.; Anant, P.; Jacob, J.; Yang, C. *J. Mater. Chem.* **2012**, *22*, 1504.

(9)   Chen, Z.; Lee, M. J.; Ashraf, R. S.; Gu, Y.; Albert-Seifried, S.; Nielsen, M. M.; Schroeder, B.; Anthopoulos, T. D.; Heeney, M.; McCulloch, I.; Sirringhaus, H. *Adv. Mater.* **2012**, *24*, 647.

(10)   Cortizo-Lacalle, D.; Arumugam, S.; Elmasly, S. E. T.; Kanibolotsky, A. L.; Findlay, N. J.; Inigo, A. R.; Skabara, P. J. *J. Mater. Chem.* **2012**, *22*, 11310.

(11)   Ha, J. S.; Kim, K. H.; Choi, D. H. *J. Am. Chem. Soc.* **2011**, *133*, 10364.

(12)   Sonar, P.; Singh, S. P.; Li, Y.; Soh, M. S.; Dodabalapur, A. *Adv. Mater.* **2010**, *22*, 5409.

(13)   Bronstein, H.; Chen, Z.; Ashraf, R. S.; Zhang, W.; Du, J.; Durrant, J. R.; Tuladhar, P. S.; Song, K.; Watkins, S. E.; Geerts, Y.; Wienk, M. M.; Janssen, R. A. J.; Anthopoulos, T.; Sirringhaus, H.; Heeney, M.; McCulloch, I. *J. Am. Chem. Soc.* **2011**, *133*, 3272.

(14)   Guo, X.; Puniredd, S. R.; He, B.; Marszalek, T.; Baumgarten, M.; Pisula, W.; Muellen, K. *Chem. Mater.* **2014**, *26*, 3595.

(15)   Qu, S.; Qin, C.; Islam, A.; Wu, Y.; Zhu, W.; Hua, J.; Tian, H.; Han, L. *Chem. Commun.* **2012**, *48*, 6972.

(16)   Qu, S.; Tian, H. *Chem. Commun.* **2012**, *48*, 3039.

(17)   Qu, S.; Wu, W.; Hua, J.; Kong, C.; Long, Y.; Tian, H. *J. Phys. Chem. C* **2010**, *114*, 1343.

(18)	Calvo-Castro, J.; McHugh, C. J.; McLean, A. J. *Dyes and Pigments* **2015**, *113*, 609.

(19)	Calvo-Castro, J.; Warzecha, M.; Kennedy, A. R.; McHugh, C. J.; McLean, A. J. *Cryst. Growth Des.* **2014**, *14*, 4849.

(20)	Warzecha, M.; Calvo-Castro, J.; Kennedy, A. R.; Macpherson, A. N.; Shankland, K.; Shankland, N.; McLean, A. J.; McHugh, C. J. *Chem. Commun.* **2015**, *51*, 1143.

(21)	Dhar, J.; Venkatramaiah, N.; Anitha, A.; Patil, S. *J. Mat. Chem. C* **2014**, *2*, 3457.

(22)	Kim, C.; Liu, J.; Lin, J.; Tamayo, A. B.; Walker, B.; Wu, G.; Thuc-Quyen, N. *Chem. Mater.* **2012**, *24*, 1699.

(23)	Mas-Torrent, M.; Rovira, C. *Chem. Rev.* **2011**, *111*, 4833.

(24)	Reese, C.; Roberts, M. E.; Parkin, S. R.; Bao, Z. *Adv. Mater.* **2009**, *21*, 3678.

(25)	Curtis, M. D.; Cao, J.; Kampf, J. W. *J. Am. Chem. Soc.* **2004**, *126*, 4318.

(26)	Coropceanu, V.; Cornil, J.; da Silva Filho, D. A.; Olivier, Y.; Silbey, R.; Bredas, J.-L. *Chem. Rev.* **2007**, *107*, 926.

(27)	Mizuguchi, J.; Grubenmann, A.; Rihs, G. *Acta Crystallogr. Sect. B* **1993**, *49*, 1056.

(28)	Mizuguchi, J.; Grubenmann, A.; Wooden, G.; Rihs, G. *Acta Crystallogr. Sect. B* **1992**, *48*, 696.

(29)	Mizuguchi, J.; Miyazaki, T. *Zeitschrift Fur Kristallographie-New Crystal Structures* **2002**, *217*, 43.

(30)	Kwon, O.; Coropceanu, V.; Gruhn, N. E.; Durivage, J. C.; Laquindanum, J. G.; Katz, H. E.; Cornil, J.; Bredas, J. L. *J. Chem. Phys.* **2004**, *120*, 8186.

(31)	Bredas, J. L.; Beljonne, D.; Coropceanu, V.; Cornil, J. *Chem. Rev.* **2004**, *104*, 4971.

(32)	Vura-Weis, J.; Ratner, M. A.; Wasielewski, M. R. *J. Am. Chem. Soc.* **2010**, *132*, 1738.

(33)	Bredas, J. L.; Calbert, J. P.; da Silva, D. A.; Cornil, J. *Proc. Natl. Acad. Sci.U.S.A* **2002**, *99*, 5804.

(34)	Cockroft, S. L.; Perkins, J.; Zonta, C.; Adams, H.; Spey, S. E.; Low, C. M. R.; Vinter, J. G.; Lawson, K. R.; Urch, C. J.; Hunter, C. A. *Organic & Biomolecular Chemistry* **2007**, *5*, 1062.

(35)	Cockroft, S. L.; Hunter, C. A.; Lawson, K. R.; Perkins, J.; Urch, C. J. *J. Am. Chem. Soc.* **2005**, *127*, 8594.

(36)	Cozzi, F.; Cinquini, M.; Annunziata, R.; Dwyer, T.; Siegel, J. S. *J. Am. Chem. Soc.* **1992**, *114*, 5729.

(37)	Cozzi, F.; Cinquini, M.; Annuziata, R.; Siegel, J. S. *J. Am. Chem. Soc.* **1993**, *115*, 5330.

(38)	Hunter, C. A.; Sanders, J. K. M. *J. Am. Chem. Soc.* **1990**, *112*, 5525.

(39)	Hunter, C. A.; Lawson, K. R.; Perkins, J.; Urch, C. J. *Journal of the Chemical Society, Perkin Transactions 2* **2001**, 651.

(40)	Martinez, C. R.; Iverson, B. L. *Chem. Sci.* **2012**, *3*, 2191.

(41)	Sinnokrot, M. O.; Valeev, E. F.; Sherrill, C. D. *J. Am. Chem. Soc.* **2002**, *124*, 10887.

(42)	Sinnokrot, M. O.; Sherrill, C. D. *J. Am. Chem. Soc.* **2004**, *126*, 7690.

(43)	Burns, L. A.; Marshall, M. S.; Sherrill, C. D. *J. Chem. Theory Comput.* **2014**, *10*, 49.

(44)   Parrish, R. M.; Parker, T. M.; Sherrill, C. D. *J. Chem. Theory Comput.* **2014**, *10*, 4417.

(45)   Hohenstein, E. G.; Chill, S. T.; Sherrill, C. D. *J. Chem. Theory Comput.* **2008**, *4*, 1996.

(46)   Antony, J.; Alameddine, B.; Jenny, T. A.; Grimme, S. *J. Phys. Chem. A* **2013**, *117*, 616.

(47)   Grimme, S. *Angew. Chem. Int. Ed.* **2008**, *47*, 3430.

(48)   Wheeler, S. E.; Houk, K. N. *J. Am. Chem. Soc.* **2008**, *130*, 10854.

(49)   Wheeler, S. E.; Houk, K. N. *J. Chem. Theory Comput.* **2009**, *5*, 2301.

(50)   Raju, R. K.; Bloom, J. W. G.; An, Y.; Wheeler, S. E. *Chemphyschem* **2011**, *12*, 3116.

(51)   Wheeler, S. E. *CrystEngComm* **2012**, *14*, 6140.

(52)   Parrish, R. M.; Sherrill, C. D. *J. Am. Chem. Soc.* **2014**, *136*, 17386.

(53)   Sherrill, C. D. *Acc. Chem. Res.* **2013**, *46*, 1020.

(54)   Sinnokrot, M. O.; Sherrill, C. D. *J. Phys. Chem. A* **2004**, *108*, 10200.

(55)   Wheeler, S. E.; McNeil, A. J.; Müller, P.; Swager, T. M.; Houk, K. N. *J. Am. Chem. Soc.* **2010**, *132*, 3304.

(56)   Ringer, A. L.; Sinnokrot, M. O.; Lively, R. P.; Sherrill, C. D. *Chemistry – A European Journal* **2006**, *12*, 3821.

(57)   Wheeler, S. E. *Acc. Chem. Res.* **2013**, *46*, 1029.

(58)   Wheeler, S. E.; Bloom, J. W. G. *The Journal of Physical Chemistry A* **2014**, *118*, 6133.

(59)   Tauer, T. P.; Sherrill, C. D. *J. Phys. Chem. A* **2005**, *109*, 10475.

(60)   Wheeler, S. E.; Houk, K. N. *Mol. Phys.* **2009**, *107*, 749.

(61)   Xia, J. L.; Liu, S. H.; Cozzi, F.; Mancinelli, M.; Mazzanti, A. *Chemistry – A European Journal* **2012**, *18*, 3611.

(62)   Gung, B. W.; Patel, M.; Xue, X. *The Journal of Organic Chemistry* **2005**, *70*, 10532.

(63)   Gung, B. W.; Xue, X.; Reich, H. J. *The Journal of Organic Chemistry* **2005**, *70*, 3641.

(64)   Muzangwa, L.; Nyambo, S.; Uhler, B.; Reid, S. A. *The Journal of Chemical Physics* **2012**, *137*, 184307.

(65)   Cozzi, F.; Cinquini, M.; Annunziata, R.; Dwyer, T.; Siegel, J. S. *J. Am. Chem. Soc.* **1992**, *114*, 5729.

(66)   Beaujuge, P. M.; Frechet, J. M. J. *J. Am. Chem. Soc.* **2011**, *133*, 20009.

(67)   Kim, B. J.; Miyamoto, Y.; Ma, B.; Frechet, J. M. J. *Adv. Funct. Mater.* **2009**, *19*, 2273.

(68)   Metten, B.; Kostermans, M.; Van Baelen, G.; Smet, M.; Dehaen, W. *Tetrahedron* **2006**, *62*, 6018.

(69)   Nowell, H.; Barnett, S. A.; Christensen, K. E.; Teat, S. J.; Allan, D. R. *Journal of Synchrotron Radiation* **2012**, *19*, 435.

(70)   Sheldrick, G. M. *Acta Crystallographica Section A* **2008**, *64*, 112.

(71)   Spek, A. L. *Acta Crystallographica Section D-Biological Crystallography* **2009**, *65*, 148.

(72)   Zhao, Y.; Truhlar, D. G. *Theor. Chem. Acc.* **2008**, *120*, 215.

(73)   Shao, Y.; Molnar, L. F.; Jung, Y.; Kussmann, J.; Ochsenfeld, C.; Brown, S. T.; Gilbert, A. T. B.; Slipchenko, L. V.; Levchenko, S. V.; O'Neill, D. P.; DiStasio, R. A., Jr.; Lochan, R. C.; Wang, T.; Beran, G. J. O.; Besley, N. A.; Herbert, J. M.; Lin, C. Y.; Van Voorhis, T.; Chien, S. H.; Sodt, A.; Steele, R. P.; Rassolov, V. A.; Maslen, P. E.; Korambath, P. P.; Adamson, R. D.; Austin, B.; Baker, J.; Byrd, E. F. C.; Dachsel, H.; Doerksen, R. J.; Dreuw, A.; Dunietz, B. D.; Dutoi, A. D.; Furlani, T. R.; Gwaltney, S. R.; Heyden, A.; Hirata, S.; Hsu, C.-P.; Kedziora, G.; Khalliulin, R. Z.; Klunzinger, P.; Lee, A. M.; Lee, M. S.; Liang, W.; Lotan, I.; Nair, N.; Peters, B.; Proynov, E. I.; Pieniazek, P. A.; Rhee, Y. M.; Ritchie, J.; Rosta, E.; Sherrill, C. D.; Simmonett, A. C.; Subotnik, J. E.; Woodcock, H. L., III; Zhang, W.; Bell, A. T.; Chakraborty, A. K.; Chipman, D. M.; Keil, F. J.; Warshel, A.; Hehre, W. J.; Schaefer, H. F., III; Kong, J.; Krylov, A. I.; Gill, P. M. W.; Head-Gordon, M. *Phys. Chem. Chem. Phys.* **2006**, *8*, 3172.

(74)   Boys, S. F.; Bernardi, F. *Mol. Phys.* **2002**, *100*, 65.

(75)   da Silva, D. A.; Kim, E. G.; Bredas, J. L. *Adv. Mater.* **2005**, *17*, 1072.

(76)   Dunitz, J. D.; Taylor, R. *Chem. Eur. J.* **1997**, *3*, 89.

(77)   Dunitz, J. D. *Chembiochem* **2004**, *5*, 614.

(78)   Bloom, J. W. G.; Raju, R. K.; Wheeler, S. E. *J. Chem. Theory Comput.* **2012**, *8*, 3167.

(79)   Sinnokrot, M. O.; Sherrill, C. D. *J. Am. Chem. Soc.* **2004**, *126*, 7690.

(80)   Cozzi, F.; Cinquini, M.; Annuziata, R.; Siegel, J. S. *J. Am. Chem. Soc.* **1993**, *115*, 5330.

(81)   Riley, K. E.; Hobza, P. *J. Chem. Theory Comput.* **2008**, *4*, 232.

(82)   Podeszwa, R.; Bukowski, R.; Szalewicz, K. *The Journal of Physical Chemistry A* **2006**, *110*, 10345.

Intermolecular interactions and energetics in the crystalline π-π stacks and associated model dimer systems of asymmetric halogenated diketopyrrolopyrroles

Jesus Calvo-Castro,*[a] Monika Warzecha,[b] Iain D.H. Oswald,[b] Alan R. Kennedy,[c] Graeme Morris,[a] Andrew J. McLean[a] and Callum J. McHugh*[a]

[a]School of Science and Sport, University of the West of Scotland, Paisley, PA1 2BE, UK.
[b]Strathclyde Institute of Pharmacy and Biomedical Sciences, University of Strathclyde, Glasgow, G1 1XL, UK.
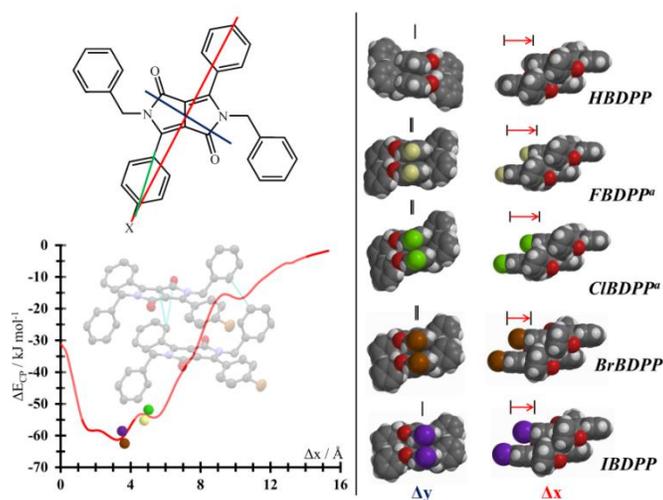
Novel structures from a series of asymmetric diketopyrrolopyrroles exhibiting slipped cofacial π-π stacks are reported. Intermonomer interactions in these systems were investigated using aligned and anti-aligned dimer models. The computed predictions are remarkably consistent with observed displacements in the crystal extracted π-π dimer equivalents, offering insight into the role of intermolecular contacts in stabilising crystal structures involving this molecular motif.